Comparison of Drusen Area Detected by Spectral Domain Optical Coherence Tomography and Color Fundus Imaging

Zohar Yehoshua,[1] Giovanni Gregori,[1] SriniVas R. Sadda,[2] Fernando M. Penha,[1] Raquel Goldhardt,[1] Muneeswar G. Nittala,[2] Ranjith K. Konduru,[2] William J. Feuer,[1] Pooja Gupta,[1] Ying Li,[1] and Philip J. Rosenfeld[1]

[1]Bascom Palmer Eye Institute, University of Miami Miller School of Medicine, Miami, Florida
[2]Doheny Eye Institute, University of Southern California Keck School of Medicine, Los Angeles, California

PURPOSE. To compare the measurements of drusen area from manual segmentation of color fundus photographs with those generated by an automated algorithm designed to detect elevations of the retinal pigment epithelium (RPE) on spectral domain optical coherence tomography (SD-OCT) images.

METHODS. Fifty eyes with drusen secondary to nonexudative age-related macular degeneration were enrolled. All eyes were imaged with a high-definition OCT instrument using a 200×200 A-scan raster pattern covering a $6 \text{ mm} \times 6 \text{ mm}$ area centered on the fovea. Digital color fundus images were taken on the same day. Drusen were traced manually on the fundus photos by graders at the Doheny Image Reading Center, whereas quantitative OCT measurements of drusen were obtained by using a fully automated algorithm. The color fundus images were registered to the OCT data set and measurements within corresponding 3- and 5-mm circles centered at the fovea were compared.

RESULTS. The mean areas ($\pm$SD [range]) for the 3-mm circles were SD-OCT = 1.57 ($\pm$1.08 [0.03–4.44]); 3-mm color fundus = 1.92 ($\pm$1.08 [0.20–3.95]); 5-mm SD-OCT = 2.12 ($\pm$1.55 [0.03–5.40]); and 5-mm color fundus = 3.38 ($\pm$1.90 [0.39–7.49]). The mean differences between color images and the SD-OCT (color − SD-OCT) were 0.36 ($\pm$0.93) ($P = 0.008$) for the 3-mm circle and 1.26 ($\pm$1.38) ($P < 0.001$) for the 5-mm circle measurements. Intraclass correlation coefficients of agreements for 3- and 5-mm measurements were 0.599 and 0.540, respectively.

CONCLUSIONS. There was only fair agreement between drusen area measurements obtained from SD-OCT images and color fundus photos. Drusen area measurements on color fundus images were larger than those with SD-OCT scans. This difference can be attributed to the fact that the OCT algorithm defines drusen in terms of RPE deformations above a certain threshold, and will not include small, flat drusen and subretinal drusenoid deposits. The two approaches provide complementary information about drusen.

Keywords: drusen, age-related macular degeneration, optical coherence tomography, color fundus photography, imaging

Drusen are one of the earliest clinical signs of age-related macular degeneration (AMD) and are characterized based on their texture (hard or soft), borders (distinct or indistinct), and their size: small (<63 μm), intermediate (>63 μm but <125 μm), or large (≥125 μm).[1–3] Numerous longitudinal studies have demonstrated correlations between total drusen area and the maximum drusen size, with the risk of progression to advanced AMD.[1,4–7] Large, soft, confluent drusen are associated with a higher risk for development of advanced AMD.[2,8,9]

High-quality, stereoscopic color fundus images have represented the gold standard in evaluating the severity and progression of AMD in major epidemiologic eye disease studies, such as the Age-Related Eye Disease Study (AREDS).[10] Total drusen area and maximum drusen size are estimated by visual inspection of drusen on color fundus photographs using a set of standardized circles.[11–13] However, the use of color fundus images to assess drusen burden can be an intensive effort even for trained graders at a reading center and often necessitates the use of a multigrader strategy to achieve meaningful quantitative assessments. The difficulty of grading drusen on color fundus images arises from interpatient variability of fundus pigmentation, media opacities, the variability of drusen appearance, the presence of small satellites of depigmentation consistent with atrophy, and the difficulty of detecting three-dimensional anatomic deformations that are lightly pigmented.[14] As a result, independent area measurements by different experts have been shown to present considerable variability.[13,15,16] Several algorithms have been developed for automated and semiautomated drusen analysis from color fundus images. Most of these automated drusen segmentation approaches are based on thresholding in the brightness domain, but clinical use is limited.[10,16,17]

The introduction of spectral domain optical coherence tomography (SD-OCT) has provided the opportunity to study drusen morphology. SD-OCT is able to acquire high-speed, high-resolution, high-density images that offer a good representation of the geometry of the retina and retinal pigment epithelium (RPE) in two and three dimensions. High-quality individual B-scans are able to show fine details of drusen structure and morphology[18] and estimate damage to the photoreceptor layer over the drusen.[19] Furthermore, recent studies have shown the potential of SD-OCT to quantify geometrical parameters of the RPE deformations typically associated with drusen, using manual measurement of drusen volume,[20] semiautomatic measurement of drusen area and drusen size,[21,22] and automatic detection and measurement of drusen area, height, and volume.[23–27]

To better understand the relationship between drusen defined as pigmentary changes on fundus photography and drusen defined in terms of RPE geometry, we compared the area measurements obtained using both imaging modalities. Some early work in this area suggested a good correlation between manual segmentation of drusen imaged using SD-OCT and color fundus photography,[20,21] while suggesting some important differences in what is captured by the two technologies. In contrast, we are using a fully automated algorithm developed at the Bascom Palmer Eye Institute that provides a quantitative assessment of RPE deformations and generates measurements of drusen volume and area.[23] This quantitative algorithm was shown to provide highly reproducible measurements of drusen area and drusen volume, and it has been used to monitor changes in drusen volume and area over time.[28] Moreover, a version of this algorithm is now commercially available (Cirrus high-definition [HD] OCT instrument, with software version 6.0; Carl Zeiss Meditec, Dublin, CA). The purpose of this study was to compare the drusen areas obtained using this automated SD-OCT algorithm with drusen areas measured on color fundus images by certified graders at a reading center.

METHODS

This prospective study was approved by the institutional review board of the University of Miami Miller School of Medicine and was compliant with the Health Insurance Portability and Accountability Act of 1996. The patients were recruited from the retina service at the Bascom Palmer Eye Institute between January 2, 2007 and January 2, 2009. Each patient signed an informed consent. The Bascom Palmer Eye Institute retina faculty confirmed the clinical diagnosis of nonexudative AMD. Digital photography, fluorescein angiography, and OCT images were obtained to document the absence of Choroidal Neovascularization (CNV) prior to including patients in the study. Eyes with geographic atrophy were excluded from this study. Patients with other concomitant retinal pathologies, including pathologic myopia, diabetic retinopathy, hypertensive retinopathy, and central serous chorioretinopathy, were excluded.

The Cirrus HD-OCT instrument (Carl Zeiss Meditec) was used in this study. Macular cube scans were obtained after pupil dilatation using one drop of 2.5% phenylephrine hydrochloride and 1% tropicamide. Each eye was imaged five separate times in a single session using a raster scan protocol (200 × 200 A-scans). This protocol resulted in the acquisition of an SD-OCT data set consisting of 40,000 uniformly spaced A-scans organized as 200 A-scans in each B-scan and as 200 horizontal B-scans in each raster array. Each scan covered a retinal area of 6 mm × 6 mm centered on the fovea. A single experienced operator, who assessed the quality of the scan

during its acquisition, performed all scans. Whenever possible, at the time of acquisition, an effort was made to exclude data sets with poor signal strength or with significant motion artifacts. The patient was repositioned during the scanning session as necessary, but there was no specific requirement to reset the patient or the instrument after acquiring each of the five separate data sets.

After acquisition, one of the authors reviewed each scan. Scans with signal strength < 7, as well as scans presenting clear evidence of motion artifacts, were categorized as low-quality scans and excluded from further analysis. For each eye, the scan with the best image quality was selected for this study. If there were several scans of similar quality, one was randomly chosen.

The raw OCT data sets were exported to a personal computer and analyzed as previously described.[23] The position of the fovea was determined manually by scanning through the OCT data set and finding the spot where the geometry of the inner retinal layers best matched the known anatomic configuration in the fovea. A proprietary algorithm was used to find the RPE and the RPE floor. The RPE floor is an extrapolated virtual RPE surface representing the geometry of an RPE free of the local deformations associated with drusen and the difference between the actual RPE segmentation and the RPE floor defines the drusen thickness map.[23] The drusen area and volume measurements were then obtained for the macular areas within circles centered on the fovea with diameters of 3 mm (C3) and 5 mm (C5) as well as for the full data set.[23]

Each SD-OCT data set was registered to the corresponding color fundus image using the OCT fundus image (OFI) and the en face retinal vascular patterns. Ad hoc software was developed[29] to register the color fundus photographs to the OFIs. This software also identified regions on the color fundus images matching the 3- and 5-mm circles centered at the fovea on the SD-OCT data sets (Fig. 1). The results of the automatic registration were reviewed by one of the authors and manual adjustments were made if the original registration was deemed not satisfactory. The drusen within the 3- and 5-mm circles on the color fundus images were then manually outlined and measured by trained, certified drusen graders at the Doheny Image Reading Center (DIRC).

The corresponding measurements of drusen area from OCT and color photo were compared using the paired t-test. Agreement between OCT and color photo areas is summarized by the intraclass correlation coefficient. All analyses were performed with a commercial analytical software program (SPSS V19; SPSS, Inc., Chicago, IL).

RESULTS

Fifty eyes from 38 patients with a clinical diagnosis of nonexudative AMD were enrolled. Measurements from the C3 and the C5 regions, from both OCT and digital color photos, were obtained for all eyes. In general, the measurements for the drusen area from the color fundus were larger than those from SD-OCT (Fig. 2). Mean drusen area measurements for the 3-mm circles (±SD [range]) were 1.57 mm² (±1.08 [0.03–4.44]) for the SD-OCT scan and 1.92 mm² (±1.08 [0.20–3.95]) for the color fundus image. For the 5-mm circles, the measurements were 2.12 mm² (±1.55 [0.03–5.40]) for the SD-OCT scan and 3.38 mm² (±1.90 [0.39–7.49]) for the color fundus image. The mean differences between the area measurements on the color fundus images and SD-OCT scans were statistically significant ($P = 0.008$ for the 3-mm circle and $P < 0.001$ for the 5-mm circle). The intraclass correlation
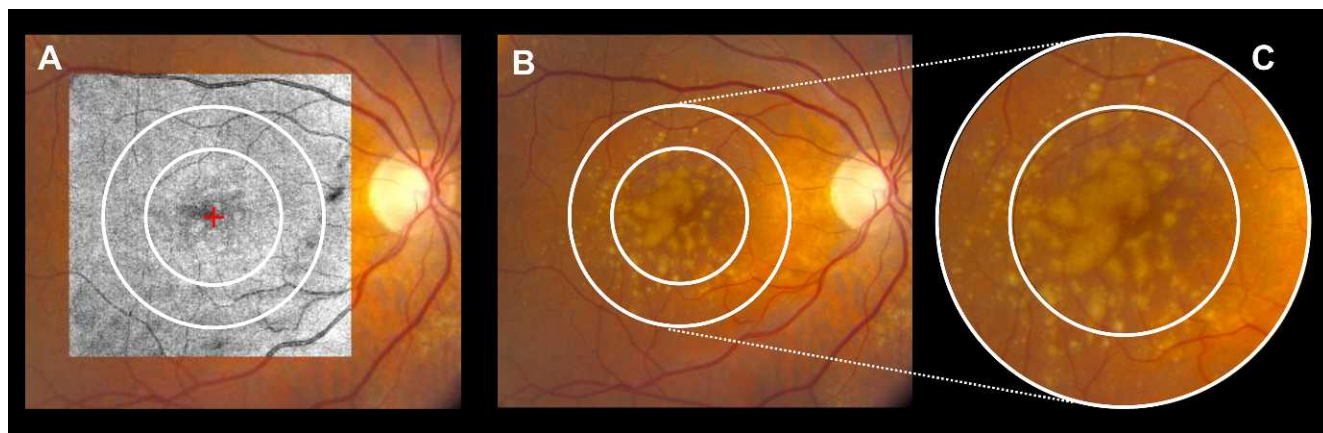
Investigative Ophthalmology & Visual Science

FIGURE 1. Registration of the SD-OCT fundus image on a color fundus photo with corresponding registration of the 3- and 5-mm circles centered on the fovea. (**A**) Registration of the OCT fundus image to the color fundus image. The foveal center is marked by the *red cross* on the OCT fundus image and the 3- and 5-mm *white circles* are centered on the foveal center. (**B**) Color fundus photo with the registered 3- and 5-mm circles. (**C**) The 3- and 5-mm circles used by the reading center for the manual outlining of drusen.

coefficients of agreement for the 3- and 5-mm measurements were 0.599 and 0.540, respectively.

Typically, but not always, the SD-OCT drusen maps captured a subset of the drusen outlined on fundus photography (Fig. 3). The disagreements between the maps could be classified into one of three different types. Areas of hypopigmentation on the color fundus image outlined as drusen by the manual graders may correspond to areas of RPE elevation not identified as drusen by the SD-OCT algorithm (Fig. 4) because these elevations were below the detection threshold (i.e., within the algorithm tolerance) or because of segmentations errors. We also found hypopigmented areas outlined as drusen by the graders that did not correspond to appreciable RPE elevation on SD-OCT (Figs. 3–5). Finally, there were examples of areas not outlined by the graders on the color fundus image that were detected by the OCT drusen map and clearly corresponded to areas of RPE elevation (Fig. 5).

DISCUSSION

In this study, area measurements of drusen within a 3- and a 5-mm circle centered at the fovea identified by experienced graders on color fundus images were found to be typically greater than the area measurements obtained using SD-OCT imaging and an automated detection algorithm. The difference in these measurements can be explained by the fact that drusen are defined on color fundus imaging based on macular pigment abnormalities, whereas drusen are defined on SD-OCT images by their deformation of the RPE geometry. As mentioned above, there were three types of situations that accounted for the disagreements between the measurements on color fundus images and the measurements on OCT data sets. The most common reason for the discrepancy was the identification of drusen on fundus images that did not significantly elevate the RPE. These include drusen that correspond to small RPE deformations seen in the OCT images
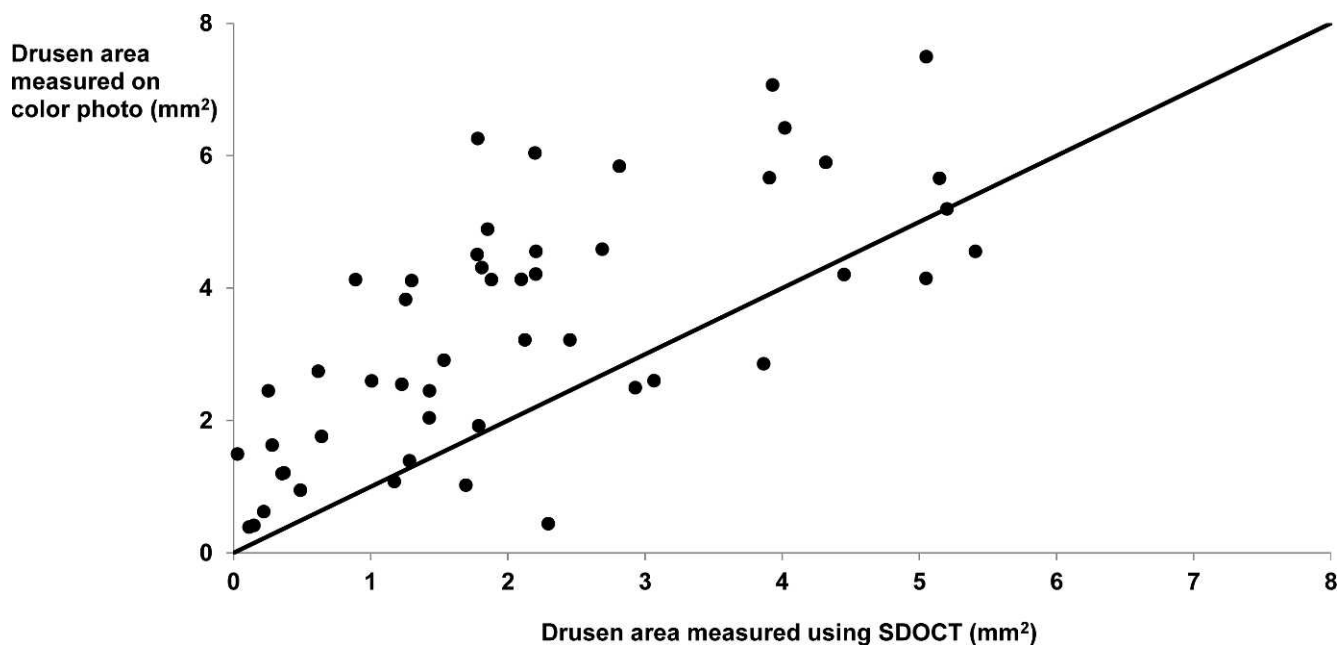

FIGURE 2. Scatterplot representing the relationship between drusen areas measured on color photos and drusen areas measured using the SD-OCT automated algorithm (5-mm *circle* only).
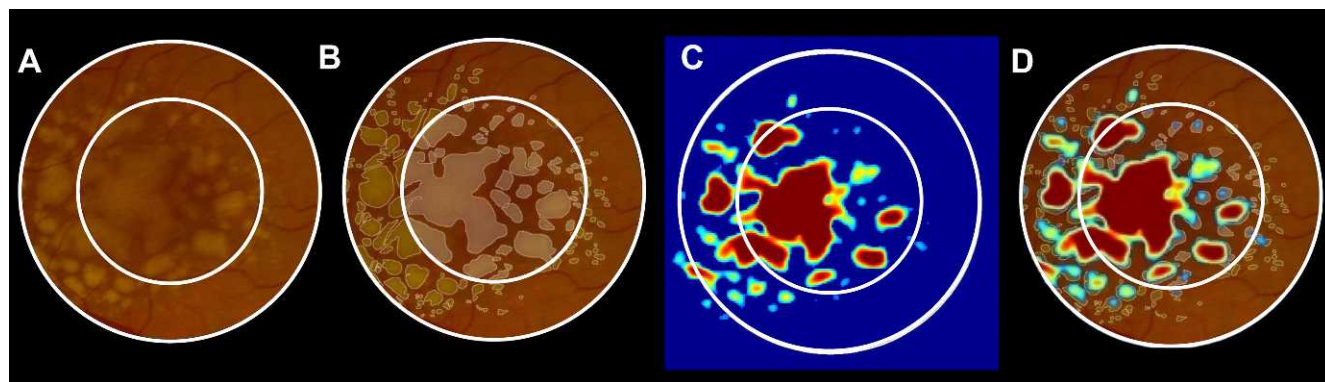
FIGURE 3. An example of good agreement between drusen areas manually measured on a color fundus photo and automatically measured by the SD-OCT algorithm. (**A**) Color fundus photo with 3- and 5-mm circles. (**B**) Manual drusen outlines performed by the reading center (drusen area 3.46 mm^2 [3 mm], 5.65 mm^2 [5 mm]). (**C**) Drusen map obtained using the automated algorithm (drusen area 3.47 mm^2 [3 mm], 5.14 mm^2 [5 mm]). (**D**) Overlay of the automated and manual drusen maps showing that SD-OCT algorithm did not identify the majority of the hypopigmented areas on the color fundus image outlined as drusen by the graders.

and might possibly be detected by a more sensitive algorithm, as well as drusen for which the OCT images show no appreciable RPE deformation. The SD-OCT drusen detection algorithm used in this study incorporates a threshold of 19.5 μm (10 pixels) to identify significant elevations of the RPE above the virtual RPE floor.[23] This threshold was set as a tradeoff between the sensitivity of the algorithm and the signal noise associated with the RPE and RPE floor segmentations. This SD-OCT algorithm will fail to detect drusen that are below the threshold, as well as flat drusen or subretinal drusenoid deposits that are located above the RPE.[30] However, the algorithm can detect RPE deformations that are not immediately evident on fundus photography. Moreover, SD-OCT imaging can provide new drusen parameters such as drusen volume and drusen height,[20–24] drusen ultrastructure,[18] and abnormalities of the outer retinal layers over drusen.[19] For these reasons, SD-OCT imaging is complementary to the grading of drusen seen on of color fundus images.

Previous studies of drusen measurements made by using manual or manually adjusted segmentation of the SD-OCT data sets appeared to correlate well with fundus photography. Freeman et al.[20] used manual segmentation of a subset of the B-scans in SD-OCT images to determine the correlation between interpolated drusen volume and drusen area from fundus photography. Jain et al.[21] found a good agreement between color fundus and manually adjusted SD-OCT measurements

when comparing parameters such as maximum drusen diameter and mean drusen area. Overall, they reported a good pixel-to-pixel correspondence between lesions that were classically classified as drusen on color fundus photos and SD-OCT findings. The mean agreement between the two imaging modalities was 82% of total image pixels. The most common areas of disagreement occurred at drusen margins, whereas 10% of the area of disagreement was represented by areas identified as drusen on color fundus photographs with no corresponding finding on SD-OCT images. They found a smaller incidence of drusen identified using SD-OCT but without corresponding pigmentary changes on the color images. Jain et al.[21] also reported a trend toward greater detection of smaller drusen by color fundus photography than by OCT images. These results show that there can be good agreement between drusen measurements on fundus photography and OCT images, at least theoretically, although there are some clear differences between the anatomic features assessed by the two modalities. However, manual segmentation of drusen is costly and time consuming. In contrast, an automated algorithm provides a fast and reproducible approach for identifying and following drusen.

It is not surprising that our results using a fully automated algorithm show a somewhat worse agreement, between drusen measurements on fundus photography and SD-OCT images, than the studies mentioned above. It should be kept in
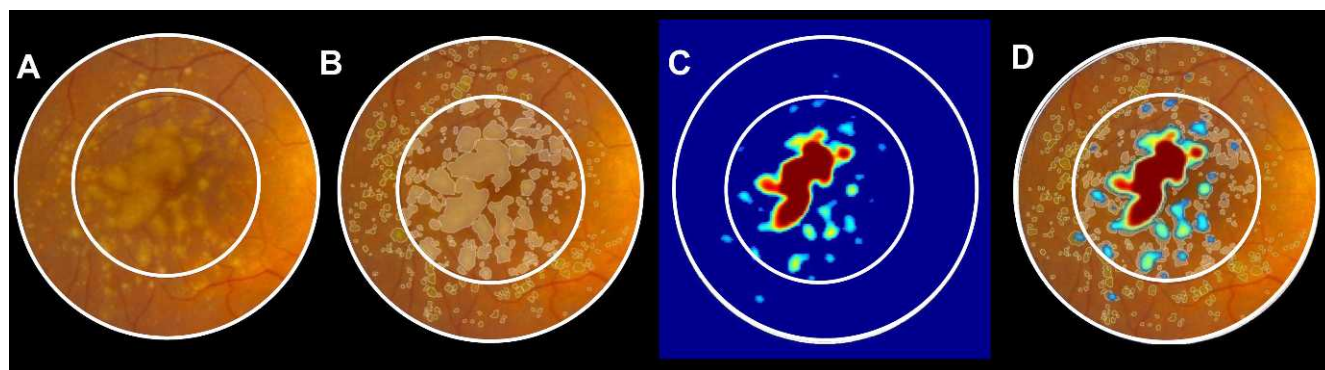

FIGURE 4. An example of manually measured drusen from the color fundus photo having a larger area than drusen measured using the automated SD-OCT algorithm. (**A**) Color fundus photo with 3- and 5-mm circles centered on the fovea. (**B**) Manual outlines of drusen performed by the reading center (drusen area 3.03 mm^2 [3 mm], 4.13 mm^2 [5 mm]). (**C**) SD-OCT drusen map with the 3- and 5-mm circles centered on the fovea (drusen area 1.85 mm^2 [3 mm], 1.88 mm^2 [5 mm]). (**D**) Overlay of the automated and manual drusen maps showing that the SD-OCT algorithm did not identify the majority of the hypopigmented areas on the color fundus image outlined as drusen by the graders.
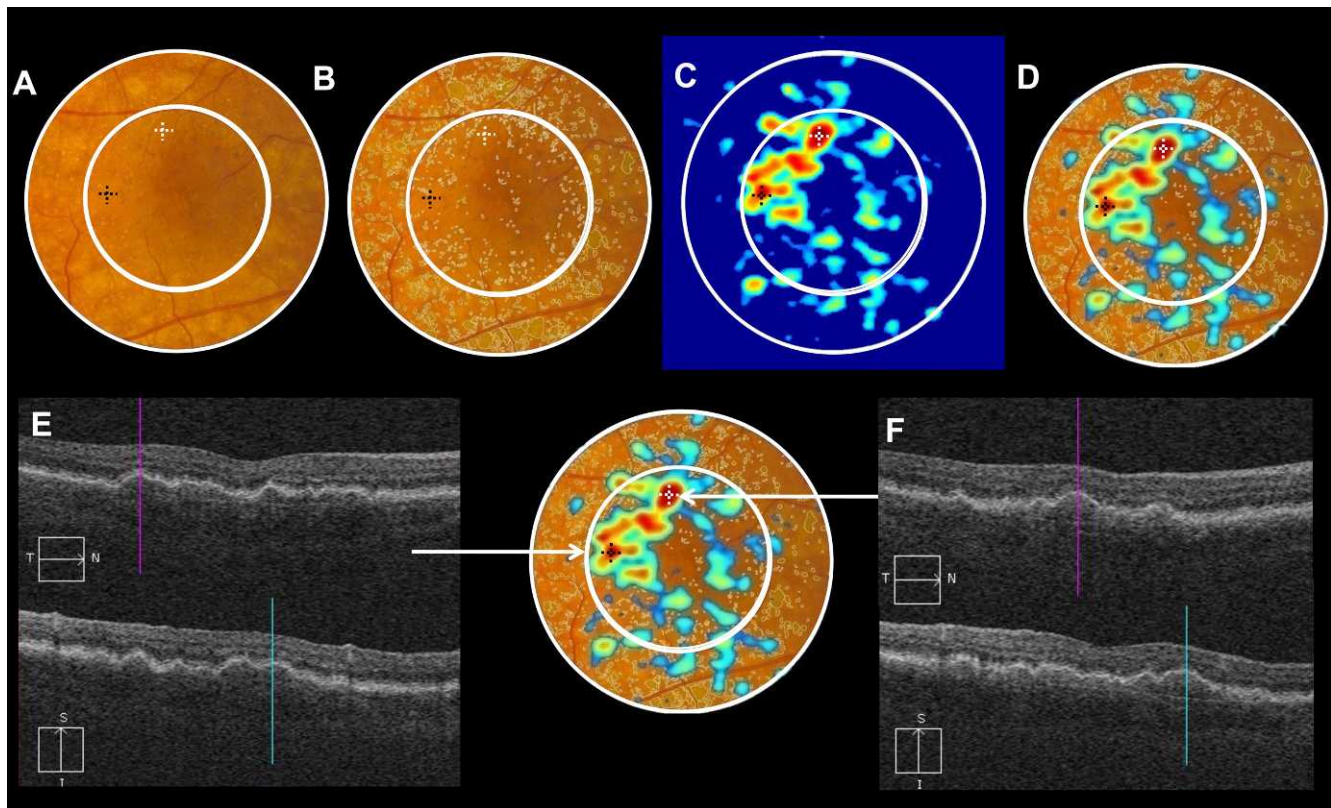
FIGURE 5. An example of manually measured drusen from the color fundus photo having a smaller area than drusen measured using the automated SD-OCT algorithm. (**A**) Color fundus photo with 3- and 5-mm circles centered on the fovea. (**B**) Manual outlines of drusen performed by the reading center (drusen area 0.86 mm² [3 mm], 2.04 mm² [5 mm]). Note, in the absence of stereoscopic information, poorly demarcated broad areas of depigmentation within the 3-mm circle, could not be identified as drusen by the graders. (**C**) SD-OCT drusen map with the 3- and 5-mm circles centered on the fovea (drusen area 3.59 mm² [3 mm], 5.34 mm² [5 mm]). The cross-hairs identify area on the drusen map where the RPE is elevated and does not correlate with typical drusen seen on the color photo. (**D**) Overlay of the automated and manual drusen maps showing that the SD-OCT algorithm identified a larger area of drusen and RPE elevation than the areas identified on the color fundus image outlined by the graders. (**E**) SD-OCT B-scan through the bottom area of disagreement (*black cross-hairs*). (**F**) SD-OCT B-scan through the top area of disagreement (*white cross-hairs*).

mind that such an algorithm, in addition to missing subthreshold drusen, might generate both some false-positive and some false-negative results because of segmentation artifacts. Furthermore, subretinal drusenoid deposits or reticular pseudodrusen will be ignored. Although reticular pseudodrusen may be confused with more typical drusen on color fundus imaging, SD-OCT imaging clearly differentiates between these types of pigmentary alterations.[30] Moreover, the color photographs that were manually segmented in this study were monoscopic. It is possible that grading of stereoscopic photographs could yield better agreement with OCT, by improving the ability to discriminate relatively flat areas of depigmentation from areas of RPE elevation. Despite these limitations, it is clear that our algorithm on the whole produces meaningful, reproducible measurements of the drusen load in a given eye. These measurements are particularly representative for the medium and larger size drusen, which may be the most clinically meaningful features for disease progression. It should be mentioned that Iwama et al.[27] discussed the relationship between digital photography and SD-OCT area measurements using a somewhat different fully automated algorithm. However, they addressed agreement only in terms of discrete AREDS classification, which is inherently a rather coarse scale. They also reported difficulties detecting small drusen, considering different choices for the noise threshold. It is possible that more accurate automated drusen measurements might be achieved by using polarization-sensitive OCT

instruments and algorithms taking advantage of the special polarization properties of the RPE.[25]

Automated SD-OCT algorithms have the ability to reliably and reproducibly measure significant RPE deformations. Such algorithms may be useful in developing improved severity scales to predict disease progression and in clinical trials as novel endpoints such as the effect on drusen volume and area when testing therapies that may affect progression to nonexudative AMD. The widespread availability of this particular algorithm on the Cirrus HD-OCT instrument (software version 6.0; Carl Zeiss Meditec) provides the clinician with a rapid, reproducible, quantitative approach for following normal disease progression in patients with nonexudative AMD.

Acknowledgments

References

1. Klein R, Klein BE, Tomany SC, Meuer SM, Huang GH. Ten-year incidence and progression of age-related maculopathy: The Beaver Dam Eye Study. *Ophthalmology*. 2002;109:1767–1779.

2. Ferris FL, Davis MD, Clemons TE, et al. A simplified severity scale for age-related macular degeneration: AREDS Report No. 18. *Arch Ophthalmol*. 2005;123:1570–1574.

3. Seddon JM, Sharma S, Adelman RA. Evaluation of the clinical age-related maculopathy staging system. *Ophthalmology*. 2006;113:260–266.

4. Bressler SB, Maguire MG, Bressler NM, Fine SL. Relationship of drusen and abnormalities of the retinal pigment epithelium to the prognosis of neovascular macular degeneration. The Macular Photocoagulation Study Group. *Arch Ophthalmol*. 1990;108:1442–1447.

5. Davis MD, Gangnon RE, Lee LY, et al. The Age-Related Eye Disease Study severity scale for age-related macular degeneration: AREDS Report No. 17. *Arch Ophthalmol*. 2005;123:1484–1498.

6. van Leeuwen R, Klaver CC, Vingerling JR, Hofman A, de Jong PT. The risk and natural course of age-related maculopathy: follow-up at 6 1/2 years in the Rotterdam study. *Arch Ophthalmol*. 2003;121:519–526.

7. Wang JJ, Foran S, Smith W, Mitchell P. Risk of age-related macular degeneration in eyes with macular drusen or hyperpigmentation: the Blue Mountains Eye Study cohort. *Arch Ophthalmol*. 2003;121:658–663.

8. Klein R, Klein BE, Knudtson MD, Meuer SM, Swift M, Gangnon RE. Fifteen-year cumulative incidence of age-related macular degeneration: the Beaver Dam Eye Study. *Ophthalmology*. 2007;114:253–262.

9. Pauleikhoff D, Barondes MJ, Minassian D, Chisholm IH, Bird AC. Drusen as risk factors in age-related macular disease. *Am J Ophthalmol*. 1990;109:38–43.

10. Bartlett H, Eperjesi F. Use of fundus imaging in quantification of age-related macular change. *Surv Ophthalmol*. 2007;52:655–671.

11. The Age-Related Eye Disease Study system for classifying age-related macular degeneration from stereoscopic color fundus photographs: the Age-Related Eye Disease Study Report Number 6. *Am J Ophthalmol*. 2001;132:668–681.

12. Bird AC, Bressler NM, Bressler SB, et al. An international classification and grading system for age-related maculopathy and age-related macular degeneration. The International ARM Epidemiological Study Group. *Surv Ophthalmol*. 1995;39:367–374.

13. Klein R, Davis MD, Magli YL, Segal P, Klein BE, Hubbard L. The Wisconsin age-related maculopathy grading system. *Ophthalmology*. 1991;98:1128–1134.

14. Pirbhai A, Sheidow T, Hooper P. Prospective evaluation of digital non-stereo color fundus photography as a screening tool in age-related macular degeneration. *Am J Ophthalmol*. 2005;139:455–461.

15. Shin DS, Javornik NB, Berger JW. Computer-assisted, interactive fundus image processing for macular drusen quantitation. *Ophthalmology*. 1999;106:1119–1125.

16. Smith RT, Chan JK, Nagasaki T, Sparrow JR, Barbazetto I. A method of drusen measurement based on reconstruction of fundus background reflectance. *Br J Ophthalmol*. 2005;89:87–91.

17. Friberg TR, Huang L, Palaiou M, Bremer R. Computerized detection and measurement of drusen in age-related macular degeneration. *Ophthalmic Surg Lasers Imaging*. 2007;38:126–134.

18. Khanifar AA, Koreishi AF, Izatt JA, Toth CA. Drusen ultrastructure imaging with spectral domain optical coherence tomography in age-related macular degeneration. *Ophthalmology*. 2008;115:1883–1890.

19. Schuman SG, Koreishi AF, Farsiu S, Jung SH, Izatt JA, Toth CA. Photoreceptor layer thinning over drusen in eyes with age-related macular degeneration imaged in vivo with spectral-domain optical coherence tomography. *Ophthalmology*. 2009;116:488–496.

20. Freeman SR, Kozak I, Cheng L, et al. Optical coherence tomography-raster scanning and manual segmentation in determining drusen volume in age-related macular degeneration. *Retina*. 2009;30:431–435.

21. Jain N, Farsiu S, Khanifar AA, et al. Quantitative comparison of drusen segmented on SD-OCT versus drusen delineated on color fundus photographs. *Invest Ophthalmol Vis Sci*. 2010;51:4875–4883.

22. Yi K, Mujat M, Park BH, et al. Spectral domain optical coherence tomography for quantitative evaluation of drusen and associated structural changes in non-neovascular age-related macular degeneration. *Br J Ophthalmol*. 2009;93:176–181.

23. Gregori G, Wang F, Rosenfeld PJ, et al. Spectral domain optical coherence tomography imaging of drusen in nonexudative age-related macular degeneration. *Ophthalmology*. 2011;118:1373–1379.

24. Schlanitz FG, Ahlers C, Sacu S, et al. Performance of drusen detection by spectral-domain optical coherence tomography. *Invest Ophthalmol Vis Sci*. 2010;51:6715–6721.

25. Schlanitz FG, Baumann B, Spalek T, et al. Performance of automated drusen detection by polarization-sensitive optical coherence tomography. *Invest Ophthalmol Vis Sci*. 2011;52:4571–4579.

26. Chiu SJ, Izatt JA, O'Connell RV, Winter KP, Toth CA, Farsiu S. Validated automatic segmentation of AMD pathology including drusen and geographic atrophy in SD-OCT images. *Invest Ophthalmol Vis Sci*. 2012;53:53–61.

27. Iwama D, Hangai M, Ooto S, et al. Automated assessment of drusen using three-dimensional spectral-domain optical coherence tomography. *Invest Ophthalmol Vis Sci*. 2012;53:1576–1583.

28. Yehoshua Z, Wang F, Rosenfeld PJ, Penha FM, Feuer WJ, Gregori G. Natural history of drusen morphology in age-related macular degeneration using spectral domain optical coherence tomography. *Ophthalmology*. 2011;118:2434–2441.

29. Li Y, Gregori G, Knighton RW, Lujan BJ, Rosenfeld PJ. Registration of OCT fundus images with color fundus photographs based on blood vessel ridges. *Opt Express*. 2011;19:7–16.

30. Zweifel SA, Spaide RF, Curcio CA, Malek G, Imamura Y. Reticular pseudodrusen are subretinal drusenoid deposits. *Ophthalmology*. 2010;117:303–312.